Afternoon Subauroral Proton Precipitation Resulting From Ring Current—Plasmasphere Interaction

M. Spasojević[1,2], M. F. Thomsen[3], P. J. Chi[4], B. R. Sandel[5]

We investigate the occurrence of arcs of precipitating protons equatorward of and detached from the afternoon proton auroral oval and their relationship with the plasmasphere and electromagnetic ion cyclotron waves. In a four month study interval including sixteen events, we find that the detached proton arcs are more likely to occur during geomagnetically disturbed periods and specifically at times when enhanced energetic ion densities and temperature anisotropies are observed in the equatorial magnetosphere. The disturbance-time arcs tend to be located at lower magnetic latitudes and are consistently associated with plasmaspheric plumes. Conversely, arcs which occur during quiet times tend to be located at higher latitudes, and their relationship with regions of enhanced cold plasma density remains unclear. Wave data available for two of the detached arc events indicate the presence of strong ion cyclotron waves near the equator in the vicinity of the proton precipitation region.

INTRODUCTION

Although the dominant loss processes for terrestrial ring current ions are collisional, including charge exchange with the neutral geocorona and Coulomb collisions within the plasmasphere, wave-particle interactions are also believed to play an important role as they provide a mechanism for the rapid decay of the ring current during the early recovery phase of geomagnetic storms [*Kozyra et al.*, 1997]. Resonant interaction between energetic ring current ions and electromagnetic ion cyclotron (EMIC) waves results in pitch angle scattering and subsequent precipitation of the energetic ions into the upper atmosphere. Considerable attention has been given to regions of spatial overlap between energetic, anisotropic ring current ions and cold, dense plasmaspheric material that should be particularly conducive to the growth of EMIC waves [*Cornwall et al.*, 1970; *Lyons and Thorne*, 1972].

In terms of magnetospheric dynamics, global magnetospheric convection and substorms act to energize and transport plasma sheet particles into the inner magnetosphere, building up the ring current [e.g. *Fok et al.*, this volume]. Convection also acts to erode the plasmasphere, and plasmaspheric material is transported sunward [e.g., *Goldstein and Sandel*, this volume] and into the path of westward-drifting ring current ions. Previously stable energetic ions distributions encounter the cold, dense plasma, become unstable to the growth of ion cyclotron waves, and some fraction of the energetic ions are scattered into the loss cone.

The free energy for wave growth in the electromagnetic ion cyclotron instability is provided by the temperature anisotropy of energetic ring current ions ($T_{\perp} > T_{||}$). Energy and momentum exchange can occur when the Doppler shifted wave frequency matches the cyclotron frequency of the individual resonant particles. According to linear Vlasov dispersion theory, the kinetic energy of protons that

[1] Space Sciences Laboratory, University of California, Berkeley, California.
[2] now at Space, Telecommunications, and Radioscience Laboratory, Stanford University, Stanford, California.
[3] Los Alamos National Laboratory, Los Alamos, New Mexico.
[4] Institute of Geophysics and Planetary Physics, University of California, Los Angeles, California.
[5] Lunar and Planetary Laboratory, University of Arizona, Tucson, Arizona.

Title
Book Series

##.####/###GM##

can resonate with a given frequency wave decreases with increasing cold plasma density [*Kennel and Petchek*, 1966]. The wave growth rate is then proportional to the temperature anisotropy of the energetic protons and the fractional number of protons near resonance. For example, at geosynchronous orbit on the dayside, the introduction of moderate densities of cold plasma (10 to 50 cm^{-3}) can reduce the resonant proton energy so that it falls within the range of the bulk of the ring current (<200 keV), and thus, more energetic protons are available for resonance. If the energetic proton temperature anisotropy is sufficiently large, waves will grow and scatter the protons until the distribution has stabilized. The maximum amplification of the ion cyclotron waves occurs near the equatorial plane, where magnetic field values are low, and for wave normal vectors parallel to the magnetic field direction [*Thorne and Horne*, 1992]. Also, heavy ions (He^+, O^+) which are present in both the hot and cold plasma distributions significantly modify the ion cyclotron wave frequencies and growth rates including the formation of stop bands above the heavy ion gyrofrequencies [*Young et al.*, 1981; *Kozyra et al.*, 1984].

The effects of wave scattering have been including in global ring current models [e.g. *Kozyra et al.*, 1997, *Jordanova et al.*, 2001, *Khazanov et al.*, 2003]. *Jordanova et al.* [2001] developed a time-dependent global EMIC wave model to study the spatial and temporal evolution of precipitating proton fluxes during different phases of a geomagnetic storm. The most intense fluxes of precipitating protons are found along the duskside plasmapause during the storm main and early recovery phases. The global precipitation patterns move to lower L shells during the main phase as the plasmasphere is eroded and recede to larger L shells during the storm recovery as the plasmasphere refills.

Although the global impact of wave-particle interactions has not been experimentally verified, a large body of supporting observational evidence does indicate that they may at times have an important influence on the evolution of the ring current. The inner edge of the ion ring current can at times penetrate the duskside plasmasphere by 0.5 to 2 R_E [*Frank*, 1971; *LaBelle et al.*, 1988; *Burch et al.*, 2001], and numerous event studies have reported ion cyclotron waves and changes in pitch angle distributions consistent with expectations from wave scattering in this overlap region [*Williams and Lyons*, 1974; *Taylor and Lyons*, 1976; *Kintner and Gurnett*, 1977; *Mauk and McPherron*, 1980; *Young et al.*, 1981]. More recently, *Erlandson and Ukhorskiy* [2001] found a direct correlation between EMIC wave spectral density and the flux of energetic protons in the loss cone. Similarly, *Yahnina et al.* [2000] reported a close association between ground based observations of Pc1 pulsations and precipitating energetic protons.

Statistically, EMIC waves (in the range 0.1–5 Hz) have been found to be primarily a phenomenon of the outer dayside magnetosphere (L>7) [*Anderson et al.*, 1992]. However, at lower L values (L=4 to 7) the occurance as well as wave amplitude is strongly peaked in the afternoon local time sector [*Anderson et al.*, 1992; *Fraser and Nguyen*, 2000; *Erlandson and Ukhorskiy*, 2001] in the region where sunward extensions of cold plasma have been frequently observed [e.g. *Chappell*, 1974]. Although *Fraser and Nyguyen* [2000] showed that the plasmapause itself is not necessarily the primary source region for waves in this L region, the vast majority of the wave events did occur where the cold plasma density exceeded 10 cm^{-3}.

2. AFTERNOON DETACHED SUBAURORAL PROTON ARCS

Global imaging of the proton aurora by the Far Ultraviolet (FUV) Spectrographic Imager (SI) [*Mende et al.*, 2000] onboard the IMAGE satellite [*Burch*, 2000] has led to the identification of arcs of precipitating protons at latitudes equatorward of and separated from the main proton oval. The detached subauroral proton arcs appear over several hours of local time in the afternoon sector, and satellite observations magnetically connected to the detached arc confirm the presence of precipitating protons and an absence of precipitating electrons [*Immel et al.*, 2002; *Burch et al.* 2002]. The afternoon detached subauroral arcs can persist for about thirty minutes up to several hours. Thus, they are distinct from other recent observations of so-called subauroral dayside proton flashes which last only for tens of minutes and are triggered by sudden increases in solar wind dynamic pressure [*Zhang et al.* 2002; *Hubert et al.* 2003].

Wave-particle interactions within the plasmasphere have been suggested as a precipitation mechanism for the afternoon detached arcs, and in one of the reported events, 10 Nov 2000, the Magnetospheric Plasma Analyzer (MPA) [*Bame et al.*, 1993] onboard the geosynchronously orbiting 1989-046 spacecraft observed enhanced fluxes of plasmaspheric ions in the region where the equatorial extension of the subauroral arc was expected to map [*Burch et al.*, 2002]. Another event study by *Spasojević et al.* [2004] indicated that the detached arc on 18 June 2001 was directly associated with a globally observed plasmaspheric plume. Predicted by numerical modeling for many years [e.g., *Grebowsky*, 1970; *Chen and Wolf*, 1972], plasmaspheric plumes, also referred to as plasma tails, are regions of cold plasma which extend sunward from the plasmasphere and are formed during periods of enhanced magnetospheric convection. They were first observed globally by the IMAGE Extreme Ultraviolet (EUV) imager [*Burch et al.*, 2001; *Sandel et al.*, 2001]. The EUV instrument [*Sandel et*

al., 2000] images the plasmasphere by detecting 30.4-nm solar radiation resonantly scattered by plasmaspheric He^+ ions.

For the 18 June 2001 event, the assertion that the proton arc was a result of wave induced scattering was supported by two main arguments [*Spasojević et al.*, 2004]. First, the auroral arc when mapped to the magnetic equatorial plane overlapped with the plasmaspheric plume as defined by a broad region of enhanced cold plasma density observed globally by IMAGE EUV and *in situ* at geosynchronous altitude by LANL-01a MPA. Second, wave growth calculations based on MPA observations of the hot and cold plasma parameters [e.g. *Gary et al.*, 1995] indicated positive growth of the proton cyclotron instability within the plume region whereas the energetic proton distributions were stable outside the plume. The wave growth calculations suggest that subauroral proton precipitation may occur at times when the hot and cold plasma distributions are similar to those observed on 18 June 2001.

Previous studies have shown that plasmaspheric plumes form readily in the afternoon local time sector during periods of enhanced convection with cold ion densities (in the range of ~1–130 eV/q) at geosynchronous orbit commonly exceeding 40 cm^{-3} [e.g., *Moldwin et al.*, 1995; *Spasojević et al.* 2003]. However, at the time of the detached arc on 18 June 2001, the hot ion density (in the range of 0.13–45 keV/q) observed by LANL-MPA was about 1.5 to 2 times larger than the average value at the same local time under similar geomagnetic conditions ($Kp \approx 5$) [*Korth et al.*, 1999]. Hence in order to further explore the relationship between detached proton arcs and plasmaspheric plumes, we examine how often the plasma parameters at geosynchronous orbit are similar to those of 18 June 2001, and more specifically, whether subauroral detached proton arcs are also observed at those times.

The association of detached arcs with plasmaspheric plumes and corresponding wave growth calculations provide only indirect evidence that the precipitation is due to EMIC wave scattering. Thus, we also investigate observations of ion cyclotron waves by the Polar Magnetic Field Experiment (MFE) [*Russell et al.*, 1995] near the geomagnetic equator in association with detached arc events.

3. IDENTIFYING DETACHED ARC EVENTS BASED ON GEOSYNCHRONOUS PARTICLE SIGNATURES

In order to identify intervals when subauroral proton precipitation may be expected, we searched the MPA data set to find times when the hot ion moments were similar to those reported for the 18 June 2001 event. Specifically, we identified intervals during which a LANL satellite was located on the dayside, $06 > \mathrm{MLT} > 18$, and for at least 30 minutes or more MPA observed a hot ion density, n_{ih}, greater than 1 cm^{-3} and a hot ion temperature anisotropy, $A \equiv T_\perp/T_\parallel - 1$, greater than 0.25. No restrictions were placed on the cold ion density as we wanted to independently determine whether the presence of cold plasma was a necessary condition for the observation of the detached arcs. The intervals were then further restricted to times when IMAGE FUV was imaging in the northern hemisphere. We performed the search over four months of data using the two LANL satellites with the best data coverage for each month. The intervals were all from 2001, in the months March (using satellites 1989–046 and 1994–084), May (1991–080 and 1994–084), June (1991–080 and 1994–084), and July (1991–080 and 1994–084).

The months of May through July 2001 were chosen because at that time the IMAGE orbit geometry was particularly favorable for EUV imaging of the plasmasphere and long intervals of high quality images are available during each orbit. During March 2001, the Polar spacecraft crossed the magnetic equator just outside of geosynchronous orbit in the post-noon sector and thus, for portions of its orbit, was in a suitable location for monitoring wave activity associated with detached arcs. Some EUV data are also available during March 2001.

Once the intervals meeting the MPA hot ion criteria ($n_{ih} > 1$ and $A > 0.25$) were identified, we surveyed the FUV S12 images for several hours around each MPA interval in search of subauroral detached proton arcs. Figure 1 gives an overview of the arc events identified using this technique over the four month study period. Overall, 13 intervals were identified when the MPA hot ion criteria were met. Of those, 11 had detached proton arcs observed by FUV, indicated by the solid vertical lines in Figure 1. The proton arcs were not necessarily observed at the same universal time or local time sector as the MPA hot ion observations. For the remaining 2 intervals, indicated by the dotted vertical lines in Figure 1, no evidence of detached subauroral precipitation was observed, and we will show that in these two cases there was no cold plasma extending to large radial distances in the afternoon sector.

3.1 Arc Events with MPA Criteria Met

We will now explore the relationship between the subauroral proton arcs and regions of enhanced cold plasma density. For each of the 11 arc events identified as a result of the MPA search criteria ($n_{ih} > 1$ and $A > 0.25$), a characteristic FUV image was selected and the subauroral proton arc was mapped to the equatorial plane so that its location could be compared with global EUV observations of the plasmasphere as well as *in situ* cold ion density measurements along geosynchronous orbit.

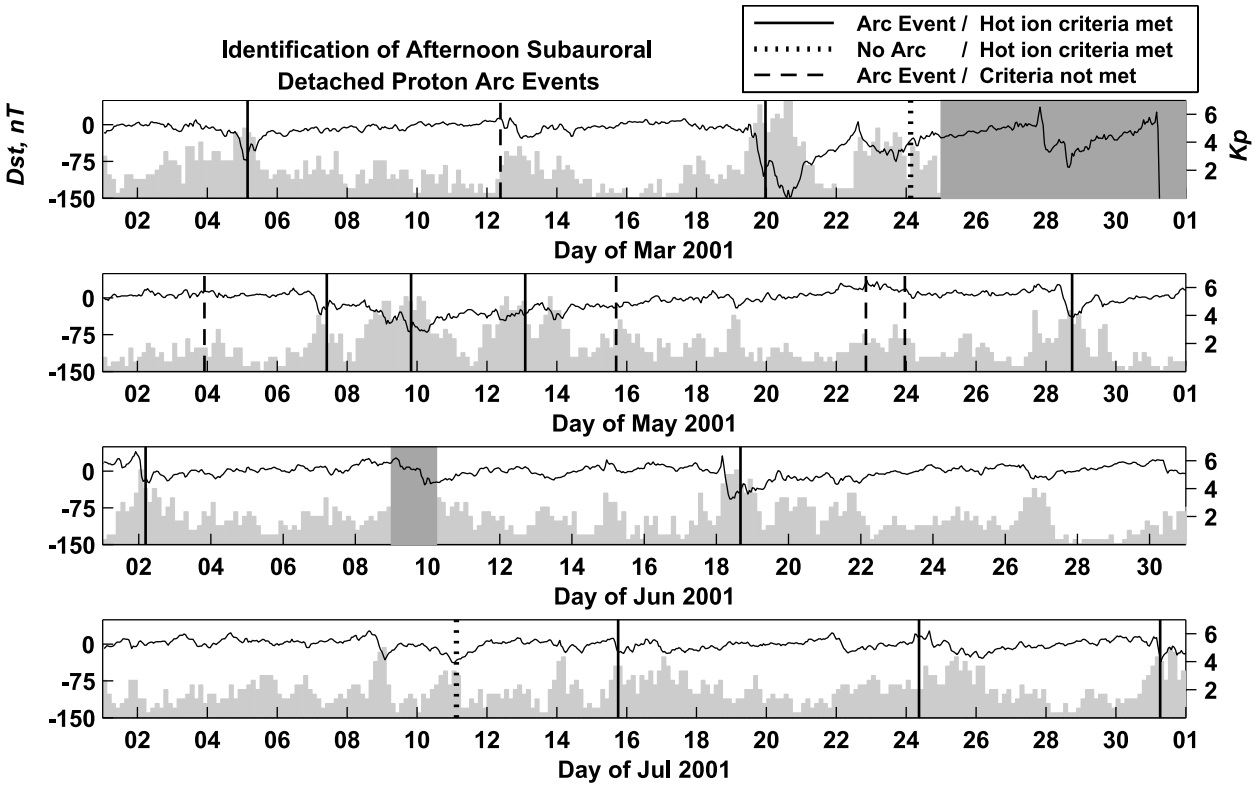

Figure 1. Geomagnetic indices *Dst* (black line) and *Kp* (light gray bars) for the months of March, May, June and July 2001. The solid vertical lines indicate times when subauroral detached proton arcs where observed and the ***in situ*** hot ion criteria were met (see text). The dotted lines indicate times when the hot ion criteria were met but no detached subauroral precipitation was observed. The dashed lines indicate arc events found when the hot ion criteria were not met. The regions covered by dark gray boxes are times when FUV data are unavailable (late Mar) or of poor quality (9–10 Jun).

3.1.1 Proton Arc Event: 05 Mar 2001 An example event from 05 Mar 2001 is shown in Figures 2–4. On that day LANL 1994-084 observed elevated hot ion densities and ion temperature anisotropies which exceeded the hot ion criteria for about an hour from 02:35 to 03:45 UT in the local time sector from 9.2 to 10.4 (segment between the two gray diamonds in Figures 2 and 4). The FUV imager observed subauroral proton precipitation in the afternoon sector for about a 3.5 hour period from about 02:45 to 05:15 UT around the time of minimum *Dst* for that disturbance interval (Figure 1). The subauroral precipitation appears to fade and rebrighten several times within the 3.5 hour period. At 03:47 UT the proton precipitation consisted of several bright spots in the afternoon sector generally extending from a magnetic latitude of ∼68º at 14 MLT to ∼60º at 17 MLT (Figure 3).

There appears to be a strong association between the mapped precipitation region and a plasmaspheric plume, as illustrated in Figure 4. Points bounding the subauroral arc were selected and mapped to the Solar Magnetic (SM) equatorial plane using the T96 magnetic field model [*Tsyganenko and Stern*, 1996] and prevailing solar wind conditions, (open squares in Figure 4). This is the same region indicated by the white dashed line in Figure 3. Overlayed are the plasmapause locations (black dots) extracted from an EUV image at 03:54 UT (center of the 10-minute integration window). The plasmapause locations were determined by selecting points along the sharp brightness gradient in the EUV image, finding the field line with the minimum apex along the line of sight to each point using the T96 magnetic field model, and tracing that field line to the SM equatorial plane. A plasmapause location was selected only at local times for which a sharp brightness gradient could be reliably identified in the EUV image [*Goldstein et al.*, 2003]. A distinct plasmaspheric plume can be seen extending sunward in the afternoon sector having been formed as result of a prolonged period of enhanced magnetospheric convection. The proton precipitation region maps within the region of the plasmaspheric plume, just inside the duskside plasmapause as determined by EUV.

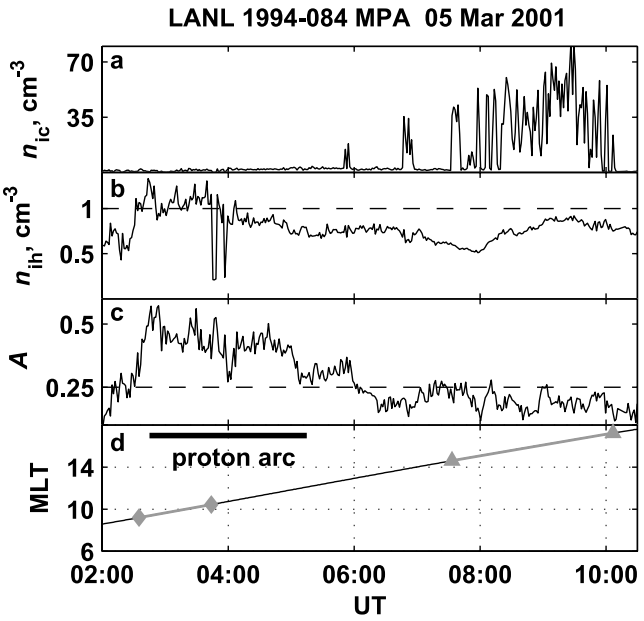

Figure 2. LANL 1994-0084 MPA observations on 05 Mar 2001 of (a) cold ion density (b) hot ion density, (c) hot ion temperature anisotropy along with (d) the satellite magnetic local time. The MPA hot ion criteria threshold is indicated by the dashed horizontal lines in (b) and (c). The MPA observations exceeded the threshold over the segment between the two gray diamonds in (d), and later that day MPA observed a plasmaspheric plume in the segment between the two gray triangles.

Unfortunately, there were no simultaneous *in situ* measurements of the hot and cold plasma parameters directly within the mapped precipitation region. However, several hours later LANL 1994-084 transversed the plume in afternoon sector as indicated by the region between the two gray triangles in Figures 2d and 4. Convection had weakened in the intervening time such that the eastern edge of the plume as measured by MPA at 10:06 UT was located at a later local time as compared to the EUV image at 03:47 UT. The average ion density across the plume was 31 cm^{-3}, and as is typically seen at geosynchronous altitude, the plume contained highly irregular density structure (Figure 2a) [*Moldwin et al.*, 1995, *Spasojević et al.*, 2003, *Goldstein et al.*, 2004].

All 11 arc events identified as a result of the MPA search criteria appear to be associated with regions of enhanced cold plasma density as determined by either global EUV images of the plasmasphere or *in situ* cold plasma density measurements at geosynchronous orbit. In characterizing association between the proton arc and regions of cold plasma, we found that the events could be broken down into one of two categories:

1. All or a significant part of the arc directly maps inside the EUV field of view and within regions of enhanced density. Events of this type include the 05 Mar 2001 event described above as well as 19 Mar 2001, 09 May 2001, 18 June 2001, 24 July 2001, and 31 July 2001.
2. The majority of the arc maps outside the EUV field of view, but EUV images indicate that a plasmaspheric plume likely extends to the mapped precipitation region. Events of this type include 07 May 2001, 13 May 2001, 28 May 2001, 02 June 2001, and 15 July 2001.

For events of both types, there are supporting MPA observations of enhanced cold ion densities in the vicinity of the mapped precipitation region.

Of the 11 proton arc events identified as a result of the MPA hot ion criteria (solid lines in Figure 1), 10 occurred during periods of at least moderately enhanced geomagnetic activity. Correspondingly, each of those 10 arcs was associated with plasmaspheric plume type extensions in the afternoon sector resulting from prolonged periods of enhanced convection. The one exception is the arc event of 24 July 2001 which occurred during a period of relatively weak geomagnetic activity. The proton arc in this event is associated with a quiet time "duskside bulge" type feature [e.g. *Carpenter*, 1970] within which the MPA instrument observed hot ion densities and temperature anisotropies in excess of the selected threshold criteria.

3.1.2 Proton Arc Event: 09 May 2001 Another example of the first type of event can be seen in Figures 5 and 6. Like

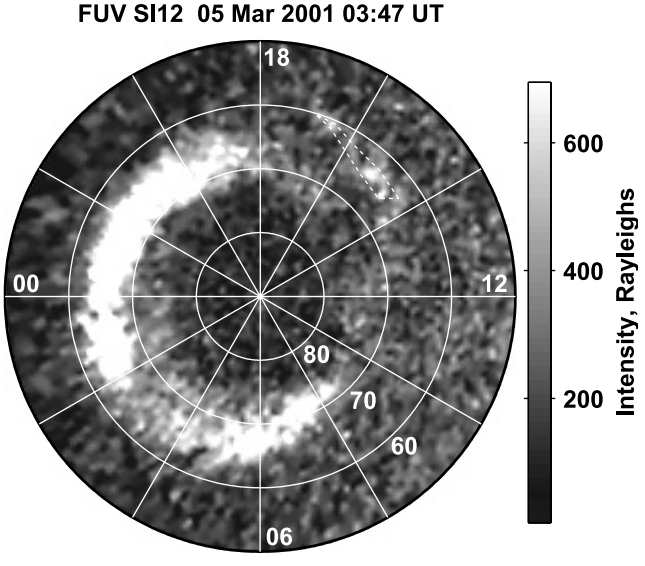

Figure 3. FUV SI12 image of the proton aurora on 05 Mar 2001 at 03:47 UT mapped onto the magnetic APEX coordinates with noon to the right. A subauroral detached proton arc can be seen in the afternoon sector between ~60° to 68°magnetic latitude, as indicated by the dashed white line.

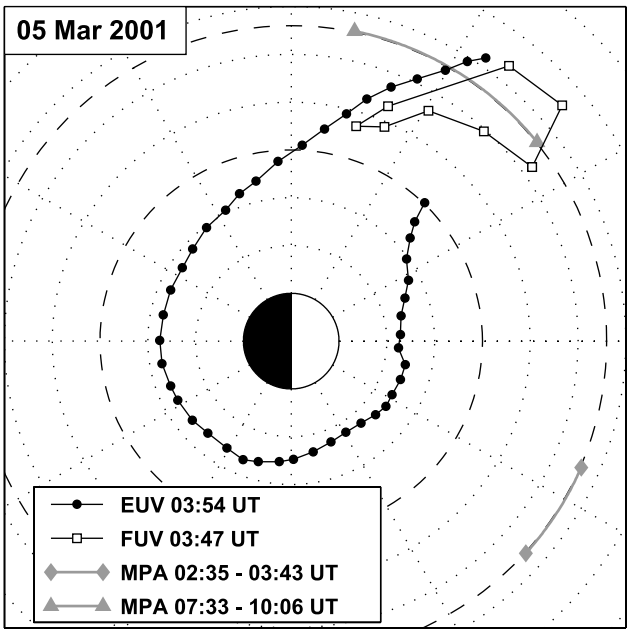

Figure 4. EUV plasmapause locations (black dots) from 05 Mar 2001 at 03:54 UT are shown along with the mapped proton precipitation region (open squares) from the FUV SI12 image at 03:47 UT. The region over which the MPA hot ion criteria were met is indicated by the gray diamonds, and MPA observations of the plasmaspheric plume were made several hours later in the region indicated by the gray triangles (as also shown in Figure 2). The sun is to the right, dotted circles are spaced 1 R_E apart, and dashed circles are at 4 and 6.6 R_E.

the previous event, on 09 May 2001 the LANL 1991-080 MPA instrument observed hot ion densities and temperature anisotropies (not shown) in excess of the selected threshold criteria in the morning sector (region between the gray diamonds in Figure 6), and there were no observations of the hot ion parameters in the afternoon sector at the time of the detached arc. Although the subauroral proton arc on 09 May 2001 was nearly twice as bright (Figure 5) as the 05 Mar 2001 event, FUV observed the arc for only about a half hour, from 19:45 to 20:15 UT. The arc was located at a later local time (17–19 MLT) and lower magnetic latitude (56º–60º) than any other event identified thus far. In addition, it is the only subauroral arc in this study which mapped completely within the EUV field of view (Figure 6) lying primarily within 4 R_E just inside the duskside plasmapause.

3.1.3 Proton Arc Event: 02 June 2001 The 02 June 2001 arc event is an example of the second type described above, where the majority of the arc maps outside the EUV field of view. The proton arc persisted from about 04:30 to 05:00 UT and maps to the equatorial plane outside of a radial distance of ~ 6 R_E (Figure 7). In addition, the arc was closer to noon than the previous examples. The EUV images at that time show a broad region of enhanced density extending from prenoon across the afternoon sector, corresponding to early stage plume development [*Spasojević et al.*, 2003]. A period of enhanced magnetospheric convection began near 00:20 UT on 02 June 2001 as determined by the the first evidence of inward motion of the nightside plasmapause and also corresponding to a strong southward turning of the interplanetary magnetic field (IMF) (indicated by upstream solar wind monitors) [*Goldstein et al.*, 2004]. The proton arc was observed after only about 4 hours of enhanced convection whereas for the two previous examples (05 Mar 2001 and 09 May 2001) the period of enhanced convection began 12 or more hours before the proton arc was observed. Thus, the observed plumes in those events (Figure 4 and 6) were narrower in local time extent as a result of the long duration of combined sunward convection and eastward corotation on the dayside.

The proton precipitation region on 02 June 2001 maps outside the EUV field of view but likely within the sunward extension of the plasmaspheric plume. At the time of the mapped images in Figure 7, the LANL 1994-084 was located near the western edge of the plasmaspheric plume (gray star in Figures 7 and 8) where the MPA instrument observed a cold ion density of ~50 cm^{-3}. MPA continued to observe plume material as it traversed the afternoon sector (region between the gray triangles). The plume began to

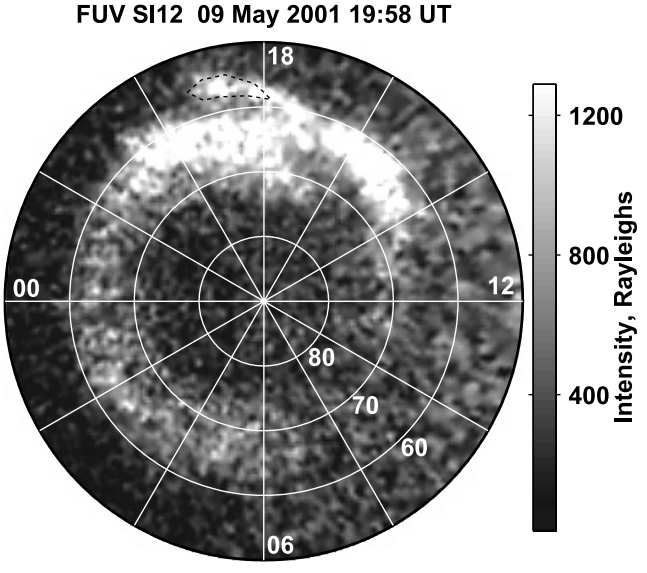

Figure 5. FUV SI12 image of the proton aurora on 09 Mar 2001 at 19:58 UT. A subauroral detached proton arc can be seen near dusk extending from ~60º near 17 MLT to ~56º near 19 MLT, as indicated by the dashed black line.

rotate eastward when convection decreased around 06:00 UT and thus LANL 1994-084 did not exit the plume until 11:53 UT. In addition, LANL 1994-084 observed enhanced hot ion densities and temperature anisotropies across much of the dayside (Figure 8b–c).

3.1.4 Proton Arc Event: 28 May 2001 A second example of a proton arc which maps outside the EUV field of view is the event of 28 May 2001 (Figure 9). Again in this event, EUV observed a well defined plume in the afternoon sector. The proton precipitation region observed by FUV maps completely outside of the EUV field of view but to a narrow local time region in what appears to be the radial extension of the plume.

3.2 MPA Criteria Met Without Subauroral Precipitation

For two of the 13 intervals which met the MPA hot ion criteria, there were no indications of subauroral proton precipitation in the FUV images. EUV images for both of these events indicate the absence of plasmaspheric plumes or bulges that extend to large radial distances in the afternoon sector.

The extracted plasmapause locations on 24 Mar 2001 from an EUV image during the interval over which MPA observed enhanced hot ion densities and temperature anisotropies is shown in Figure 10a. At this time, the average plasmapause location was at $L \approx 3.6$. A remnant of a small plume can be seen centered at $\sim$ 21 MLT. The EUV observations over the previous several days suggest that the plasmasphere was severely depleted during the large magnetic storm which occurred 19–21 Mar 2001 (Figure 1) and did not recover prior to the subsequent disturbance beginning on 22 Mar 2001. Thus, despite a period of prolonged enhanced convection, a well-defined large scale plume did not form during the second disturbance period. MPA observations on 24 Mar 2001 also confirm the absence of cold plasma at geosynchronous altitude (not shown).

The other MPA hot ion criteria interval for which no subauroral precipitation was observed is 11 July 2001. EUV images from during this time (Figure 10b) indicate that the plasmasphere was inside 4 R_E except for a slight bulge extending to 5 R_E in the afternoon sector. Prior to the EUV data shown in Figure 10b, the IMF had been southward for the past $\sim$ 18 hours, so it is somewhat puzzling that a large scale plume had not formed. One possibility is that convection electric field was effectively shielded from the inner magnetosphere on this day by the inner edge of the plasma sheet and the Region 2 field-aligned current system [e.g.,

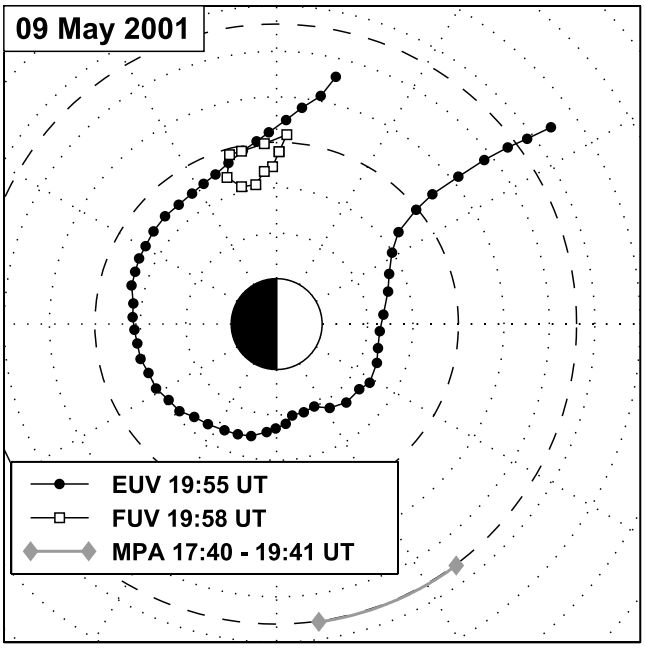

Figure 6. EUV plasmapause locations (black dots) from 09 May 2001 at 19:55 UT are shown along with the mapped proton precipitation region (open squares) from the FUV SI12 image at 19:58 UT. The region over which the MPA hot ion criteria were met is indicated by the gray diamonds.

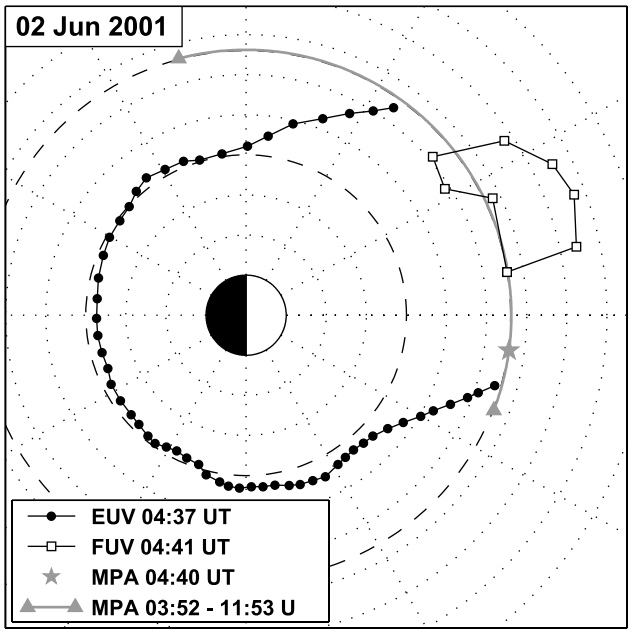

Figure 7. Plasmapause locations (black dots) and the mapped proton precipitation region (open squares) on 02 June 2001. LANL 1994-084 was at the location of the gray star at the time of the EUV and FUV observations, and MPA observed enhanced cold plasma density over the region between the gray triangles as shown in Figure 8.

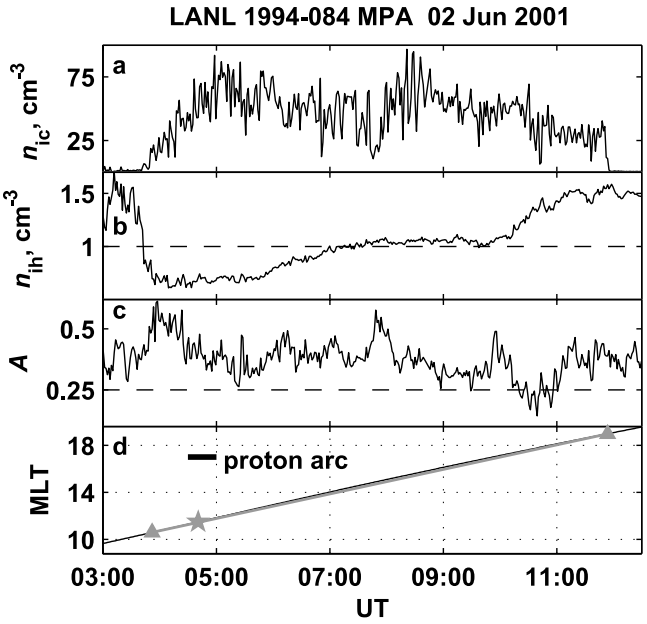

Figure 8. Same as Figure 2, except the gray star in (d) indicates the location of LANL 1994-084 at the time of the EUV and FUV observations in Figure 7.

Jaggi and Wolf, 1973]. This interpretation is supported by observations by the solar wind monitors of a gradual rotation in the IMF from northward to southward over a period of about six hours which could have allowed an effective shielding layer to be established.

Therefore, for the events of 24 Mar 2001 and 11 July 2001, it is possible that the lack of subauroral precipitation may be related to the absence of cold plasma outside ~ 4 to 5 R_E even though the hot ion parameters observed by MPA were similar to those during other subauroral detached proton arc events.

4. ADDITIONAL DETACHED ARC EVENTS

In addition to the subauroral detached arc events discussed thus far, five more arc events were found within the four month study interval at times when the *in situ* hot ion criteria were not met. These events are indicated by the dashed lines in Figure 1 and were identified as a result of a visual survey of the FUV SI12 images for the months of March, May, June and July 2001. In contrast to the arc events discussed in Section 3.1, these arc events on average occurred under quieter geomagnetic conditions and were located at higher magnetic latitudes. For each of these five events, the entire proton precipitation region maps to the equatorial plane outside of geosynchronous orbit, and thus it is not unexpected that the criteria used to identify arc events based on geosynchronous particle observations would be insufficient to identify these events. Also since the arcs map to such large radial distances, it is not possible, using EUV images and MPA observations alone, to unambiguously assess the relationship between the arcs and regions of enhanced cold plasma density for each of these events.

4.1 Proton Arc Event: 22 May 2001

One such example is 22 May 2001 as shown in Figure 11a. The detached proton arc at 20:19 UT maps to a radial distance of between 8 and 10 R_E in the pre-dusk sector. At the time of the arc, the IMAGE satellite was still at relatively low altitude such that the plasmasphere completely filled the EUV field of view. By 22:06 UT, the satellite was closer to apogee and the EUV extracted plasmapause locations indicate a large bulge in the dusk to midnight quadrant which extends to edge of the EUV field of view to at least 7–8 R_E. It is possible this bulge was collocated with the proton arc but in the subsequent two hours corotated eastward. Similarly, for the events of 12 Mar 2001, 03 May 2001, and 23 May 2001, the association with cold plasma using the existing EUV and/or MPA data is difficult to establish precisely .

4.2 Proton Arc Event: 15 May 2001

One detached arc event which is clearly unrelated to any plasmaspheric density structure occurred on 15 May 2001 (Figure 11b). The proton arc at 16:45 UT maps to a radial distance of ~ 10 R_E, further out than any other arc in this

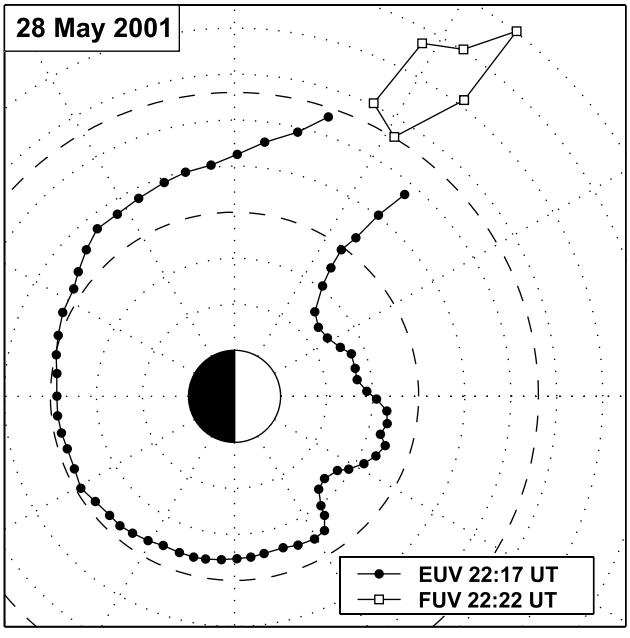

Figure 9. Plasmapause locations (black dots) and the mapped proton precipitation region (open squares) on 28 May 2001.

study. Although high quality EUV data was not available at the time the arc was present, observations at 19:02 UT indicated that the plasmasphere was devoid of any large scale bulges and the plasmapause was located at $\sim 4.5\ R_E$ in the dusk sector.

5. RELATIONSHIP BETWEEN DETACHED ARCS AND GEOMAGNETIC ACTIVITY

The spatial distribution of all 16 detached proton arc events is shown in Figure 12. Each dot is the centroid of the the mapped precipitation region determined from one FUV image during the event with the gray dots corresponding to detached arcs identified by the MPA hot ion criteria (solid lines in Figure 1) and the open dots to those that did not meet the specified criteria (dashed lines in Figure 1). As previously mentioned, the open dots map to larger radial distances. The average location of all the proton arcs events is $r = 7.4\ R_E$. There is a clear correlation between the radial distance of the mapped arc centroid and the level of geomagnetic activity as measured by the *Dst* index (Figure 13). The arcs tend to be located at lower latitudes, and thus map closer to the Earth, during geomagnetically disturbed periods. The linear correlation coefficient is 0.69 (high statistical significance). The correlation between arc radial distance and *Kp* was similar ($\rho = 0.70$). Conversely, there was no correlation found between geomagnetic activity and the local time of the arc centroid.

6. Relationship between Detached Arcs and Solar Wind Conditions

Previous studies have reported that subauroral detached proton arcs can be observed after a change from negative to positive of either the B_z or B_y component of the interplanetary magnetic field (IMF) [*Burch et al.*, 2002; *Spasojević et al.*, 2004]. As a result of either IMF transition, the main proton oval in the afternoon sector contracts poleward, while the equatorward part of the oval remains at its original latitude. Thus, a separation of several degrees in latitude is created between the new oval position and the presumably pre-existing proton arc. In addition, the previously reported detached arc events occurred during periods of relatively high solar wind dynamic pressure.

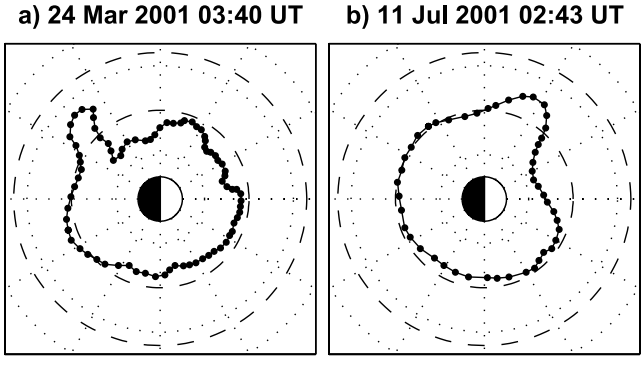

Figure 10. EUV plasmapause locations on a) 24 Mar 2001 and b) 11 July 2001 at times when MPA hot ion parameters exceeded the selected threshold, but FUV did not observe any detached subauroral precipitation. Dotted circles are 2 R_E apart and dashed circles indicate 4 and 6.6 R_E.

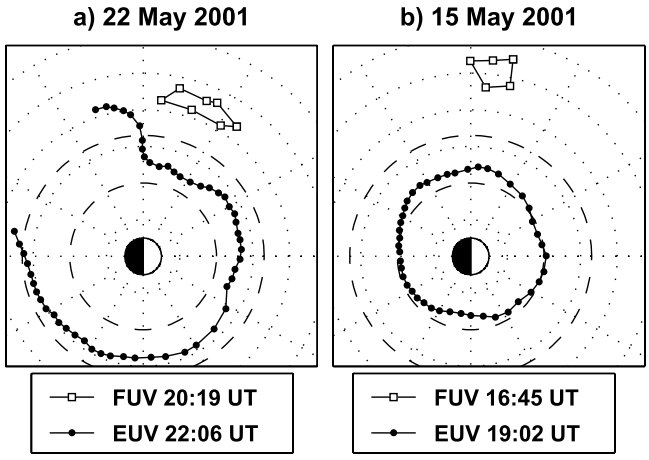

Figure 11. EUV plasmapause locations and FUV mapped precipitation regions for a) 22 May 2001 and b) 15 May 2001. The MPA hot ion criteria were not met during these detached arc events. Dotted circles are 2 R_E apart and dashed circles indicate 4 and 6.6 R_E.

To further explore the relationship between detached proton arcs and solar wind conditions, we performed a superposed epoch analysis of the parameters IMF B_z, B_y and solar wind dynamic pressure using all 16 arc events (Figure 14). The solar wind data was taken from either the ACE or WIND satellites, and the data for each event interval was appropriately time shifted to account for propagation to the magnetopause. The epoch time of 0 hours (solid vertical line) corresponds to the time the detached arc was first observed. Thus, each panel in Figure 14 represents the average value of each solar wind parameter from eight hours prior to four hours after the detached arc was first observed.

For IMF B_z, there is a clear pattern of southward IMF for about six to eight hours prior to the arc occurrence. This is not unexpected given that most of the arcs occurred during negative excursions of *Dst* and were associated with plasmaspheric plumes which form during periods of enhanced magnetospheric convection. However, at the time the arc is first observed and in the hours that follow, the average value of B_z is close to zero. In examining the 16 individual B_z records, in about half of the events, the arcs appear after a northward

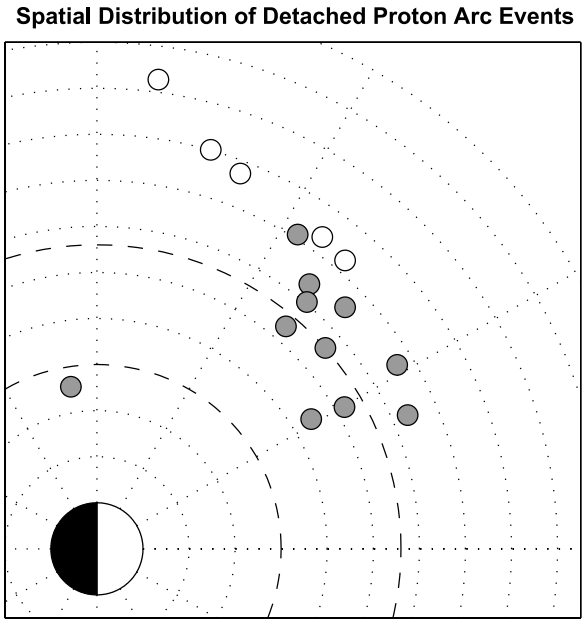

Figure 12. The spatial distribution of all 16 subauroral detached proton arcs identified in the four month study period. Each dot is the centroid of the mapped precipitation region determined from one FUV image during the each event. The gray dots are the events which were identified during intervals which the MPA hot ion criteria were met while the criteria were not met for the open circles. Dotted circles are 1 R_E apart and dashed circles indicate 4 and 6.6 R_E.

IMF turning, and there are particularly abrupt transitions for the events of 05 Mar 2001, 18 June 2001 and 31 July 2001. On the other hand, in the remaining half of the events the IMF remains southward or near zero. Thus, a negative to positive IMF B_z transition is not a necessary condition for the formation of detached proton arcs. However, the fact that some of the arcs are only visible after a northward turning, which causes the main proton oval to contract poleward, suggests that at other times ring current precipitation as a result of interaction with the plasmasphere may contribute to the equatorward portion of the auroral oval even though a distinct and detached arc is not present. There does not appear to be a systematic trend in the IMF B_y in either the superposed epoch analysis, in which the average value before and after the arc observation is close to zero, or in the inspection of the B_y records for individual events.

The detached proton arcs are in general associated with extended periods of enhanced solar wind dynamic pressure consistent with the previously reported case studies. The average dynamic pressure both before and after the arc observation is $\sim$ 3.4 nPa while the average dynamic pressure for the entire four month period is $\sim$ 2.0 nPa. Only one of sixteen arc events did not occur during elevated dynamic pressure, so while high dynamic pressure is perhaps not a necessary condition, arcs are more likely to be seen during the high pressure intervals. The afternoon detached arcs do not appear to be associated with pressure pulses such as has been reported for another class of so-called dayside subauroral proton flashes [*Zhang et al.*, 2002; *Hubert et al.*, 2003].

7. OBSERVATIONS OF ION CYCLOTRON WAVES IN ASSOCIATION WITH DETACHED ARCS

The close association between afternoon subauroral detached proton arcs and regions of cold, dense plasmaspheric material for the majority of arc events in this study supports the previous assertions of *Burch et al.* [2002] and *Spasojević et al.* [2004] that the precipitation may be due to pitch angle scattering of energetic protons by electromagnetic ion cyclotron (EMIC) waves which may preferentially be amplified in regions of enhanced cold plasma density. In addition, *Immel et al.* [this volume] reported ground observations of magnetic pulsations in the Pc1 range in association with four detached arc events. However, ion cyclotron waves are likely generated near the equatorial plane, and may be damped in the off-equatorial regions or affected by ionospheric transmission [*Fraser et al.*, 1996; *Mursula et al.*, 2000].

During March of 2001 Polar crossed the magnetic equatorial plane at radial distances of 7–8 R_E in the post-noon local time sector. We identified conjunction intervals during that month when Polar was near the magnetic equator while the IMAGE spacecraft was positioned at high northern latitudes imaging both the proton aurora and the cold plasma distribution. Fortunately, two of the three detached arc events identified in March 2001 (12 Mar 2001 and 19 Mar 2001) occurred during conjunction times. Although Polar does not pass directly through the mapped precipitation region, the Magnetic Field Experiment (MFE) observed strong EMIC

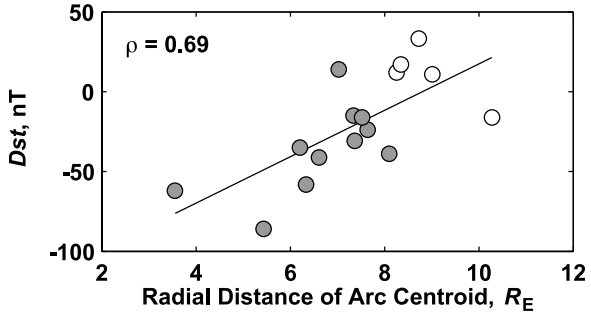

Figure 13. Correlation between the radial distance of the arc centroid and the *Dst* magnetic index at the time of the arc. The circle designations are the same as in Figure 12. The linear correlation coefficient is 0.69 (highly significant).

wave activity during both events. In analyzing the Polar MFE data for the remainder of the month, we found that there are no other periods of strong wave activity during IMAGE conjunctions, nor are there observations of detached arcs during conjunction times in the absence of waves. The third detached arc event of the month, 05 Mar 2001, did not occur during a conjunction with Polar.

7.1 Proton Arc Event with EMIC Waves: 19 Mar 2001

On 19 Mar 2001, FUV observed a detached proton arc during the main phase of a large geomagnetic storm (Figure 1). The detached arc maps to the equatorial plane directly within a plasmaspheric plume observed by EUV (Figure 15). About two hours earlier, the Polar spacecraft crossed the equatorial plane at slightly earlier local time than the mapped precipitation region. In Figure 15, the location of the Polar spacecraft from 20:00 to 22:00 UT was traced to the SM equatorial plane using the T96 magnetic field model. The magnetic field observations over that interval (Figure 16) show the presence of strong ion cyclotron waves that are confined to below the He^+ gyrofrequency (dashed line). We verified that the waves are left-hand polarized and propagate along the magnetic field direction.

7.2 Proton Arc Event with EMIC Waves: 12 Mar 2001

The detached proton arc on 12 Mar 2001 occurred near the onset of a small geomagnetic disturbance and the precipitation region at 09:16 UT maps to the equatorial plane outside of geosynchronous orbit (Figure 17). There were no EUV images available at the time of the detached arc, but about

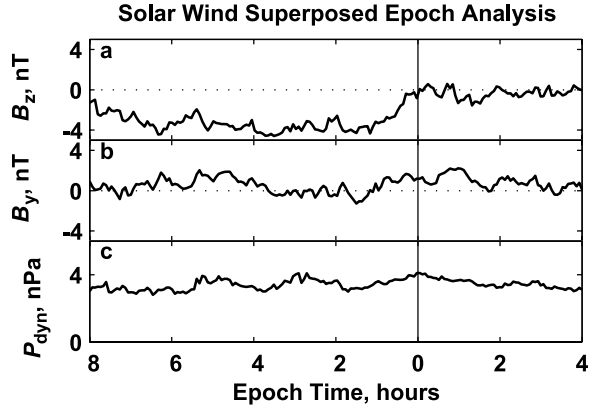

Figure 14. Superposed epoch analysis of a) IMF B_Z, b) IMF B_Y and c) solar wind dynamic pressure for all 16 subauroral detached proton arcs. The solar wind data was propagated to the magnetopause for each event, and the epoch time of 0 hours refers to the time the detached arc was first observed.

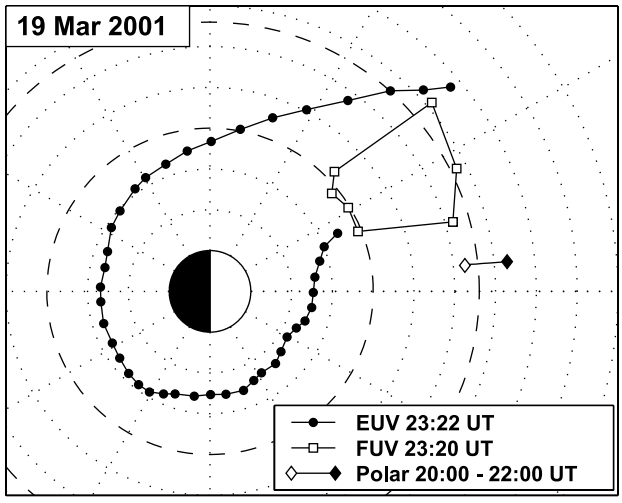

Figure 15. Plasmapause locations (black dots) and the mapped proton precipitation region (open squares) are shown for 19 Mar 2001 along with the location of the Polar spacecraft, mapped to the SM equatorial plane, for a two hour period during which MFE observed strong EMIC waves as shown in Figure 16.

five hours earlier, EUV observed a rather expanded plasmasphere with the plasmapause on the nightside extending to a radial distance of $\sim 6\ R_E$. The plasmapause location on the dayside could not be reliably identified due to sunlight contamination. The MPA instrument on LANL 1994-084 observed cold plasma with densities greater than 10 cm^{-3} in the afternoon sector (region bounded by the gray triangles in Figure 17a,b). At the time the proton arc was observed, MPA measured a cold plasma density of ~ 35 cm^{-3} just Earthward of the proton arc (location of the gray star).

From 08:15 UT to 10:00 UT, Polar MFE observed ion cyclotron waves at about the same radial distance as the mapped proton precipitation region but at an earlier local time. In this event, ion cyclotron waves were primarily above the He^+ gyrofrequency (dashed line in Figure 18) although near 08:30 UT there is some wave energy below the He^+ gyrofrequency.

In both detached arc events (19 Mar 2001 and 12 Mar 2001), the ion cyclotron waves are observed at about the same radial distance as the mapped precipitation region but Polar was at a slighter earlier magnetic local time. The difference in the wave spectra in the two events can be attributed to differences in the heavy ion content of the plasma [*Kozyra et al.*, 1984]. In the non-storm time event, 12 Mar 2001, the wave energy was above the local He^+ gyrofrequency and thus the energetic ions were likely primarily composed of protons. If a significant amount of cold plasma was present, it was also likely primarily protons. For the storm time event, 19 Mar 2001, waves above the He^+ gyrofrequency were absent and

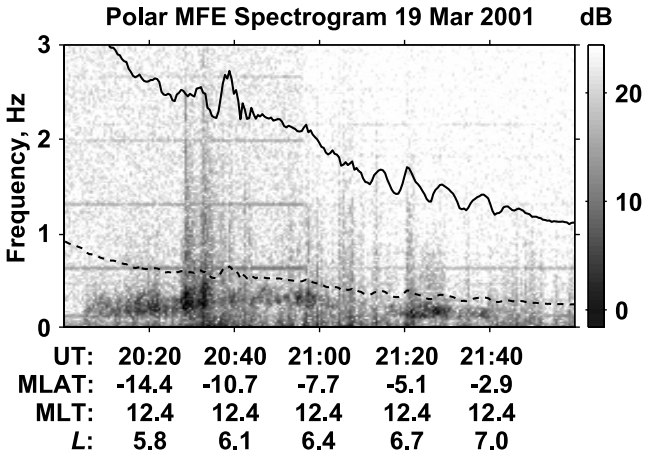

Figure 16. MFE spectrogram for the portion of the Polar orbit shown in Figure 15. The solid and dashed black lines are the H^+ and He^+ gyrofrequencies respectively. In addition to universal time, magnetic latitude, magnetic local time and *L* value (based on a dipole magnetic field) are also shown.

high fractions of heavy ions have been shown to suppress wave growth in this range. Clearly, there was a significant amount of He^+ in the plume region of the plasmasphere since EUV instrument images the He^+ distribution, but there may have also been enhanced heavy ions in the hot plasma distribution as is typical of the storm time ring current.

8. DISCUSSION

We have investigated the occurrence of afternoon subauroral detached proton arcs observed by the IMAGE FUV SI12 instrument and their relationship with regions of enhanced cold plasma density, electromagnetic ion cyclotron waves as well as geomagnetic and solar wind conditions during the months of March, May, June and July 2001.

In situ measurements of energetic ion parameters can be useful in identifying intervals when the detached proton arcs are likely to occur. Over the four month study period, we identified 13 intervals when enhanced hot ion densities and temperature anisotropy were observed at geosynchronous orbit on the dayside. FUV observed subauroral detached proton arcs during 11 of the 13 intervals. Although the exact choice of the hot ion criteria (nih $>$ 1 and A $>$ 0.25) was somewhat subjective, it was based upon measured values of 18 June 2001, a time when wave growth would have been expected based on instability calculations using the *in situ* hot and cold plasma parameters inside the mapped precipitation region [*Spasojević et al.*, 2004]. Only two of the 13 hot ion criteria intervals did not appear to have subauroral precipitation (24 Mar 2001 and 11 July 2001), and EUV and MPA observations for those events indicate that plasmasphere was rather compact and no cold plasma extended to geosynchronous orbit.

Five additional arcs were identified during intervals that did not meet MPA hot ion criteria. In general, these events occurred under quieter geomagnetic conditions and mapped to the equatorial plane well outside of geosynchronous orbit. Therefore, it is not unexpected that the criteria used to identify arc events based on geosynchronous particle observations would be insufficient to identify these events. Statistically, energetic proton distributions become more unstable to wave growth with increasing radial distance [*Anderson et al.*, 1992], but due to a lack of satellite observations outside of geosynchronous orbit, we are unable to verify this effect for these higher latitude arc events.

We found highly significant statistical correlation between the level of geomagnetic activity, using *Dst* and *Kp*, and

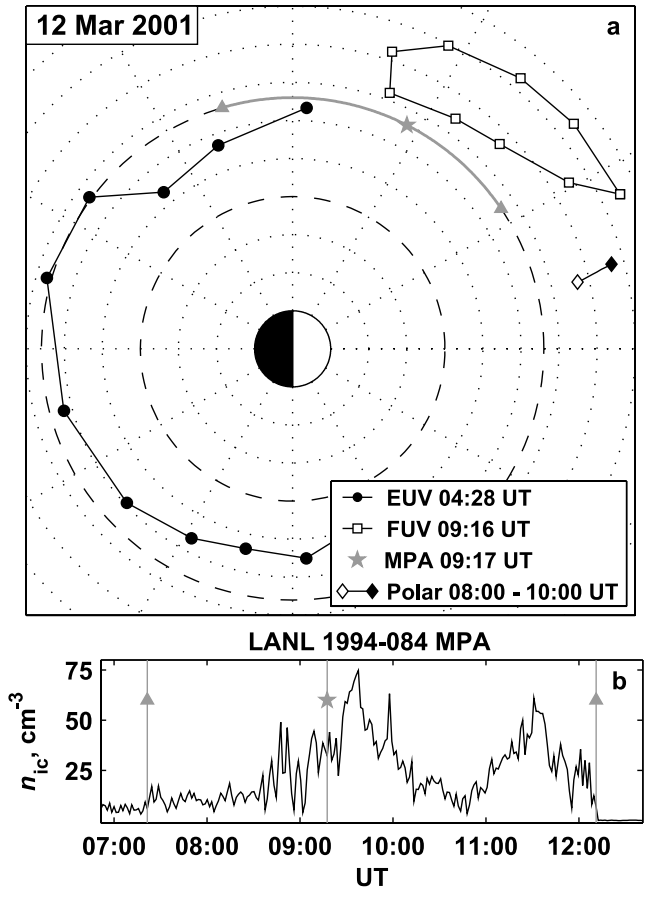

Figure 17. a) Same as Figure 15 for 12 Mar 2001. The MFE data for the segment of the Polar orbit is shown in Figure 18. Also included is the location of the LANL 1994-084 at the time of the FUV observation (gray star). b) LANL 1994-084 MPA measurements of cold ion density. MPA observed cold plasma with density $>$ 10 cm^{-3} in the region between the gray triangles in a) and b).

location of the detached arc. During disturbed conditions, the arcs tend to map in the equatorial plane to smaller radial distances (that is, the arc is located at lower magnetic latitudes) while during quiet conditions, the arcs map to larger radial distances (located at higher latitudes).

Overall, the majority of detached arc events in this study occurred during periods of moderate to strong geomagnetic disturbance. For each of the disturbance-time events, there is a clear association between the mapped proton precipitation region and a global scale plasmaspheric plume. Supporting MPA observations of cold ion densities in the range of 20–50 cm^{-3} within the plume are also available for many of these events.

In contrast, since the events which occurred under quieter conditions map further out, it is not possible to unambiguously confirm the presence of enhanced cold plasma. For the events of 12 Mar 2001, 03 May 2001, 22 May 2001, and 23 May 2001, EUV observes a large, expanded plasmasphere, typical of quiet times, and MPA observes cold plasma at geosynchronous orbit. However, it is still difficult to link these observations of cold plasma to precipitation regions that map out to $> 8\ R_E$. In addition, the 15 May 2001 detached arc event appears to be completely unrelated to any plasmaspheric structure. It is possible that the detached arcs which map to larger radial distances are still a result of wave scattering, but the wave amplification proceeds in the absence of cold plasma [*Kozyra et al.*, 1984]. Another possibility is that they may be related to detached blobs of cold plasma trapped in the outer magnetosphere in the aftermath of periods of enhanced convection [*Carpenter et al.*, 1993].

Hot-cold plasma interaction provides an attractive mechanism for the formation of the proton arcs since it could explain why the arcs appear detached from the main proton auroral oval. In absence of cold plasma, the conditions for wave growth become more favorable as the magnetopause is approached due to reduced magnetic field strength and increased temperature anisotropy resulting from drift shell splitting. Enhanced cold plasma in the middle magnetosphere (5–7 R_E) might provide an isolated region closer to the Earth where wave growth and scattering is enhanced. The proton precipitation region in the ionosphere would then appear isolated and detached from the main oval.

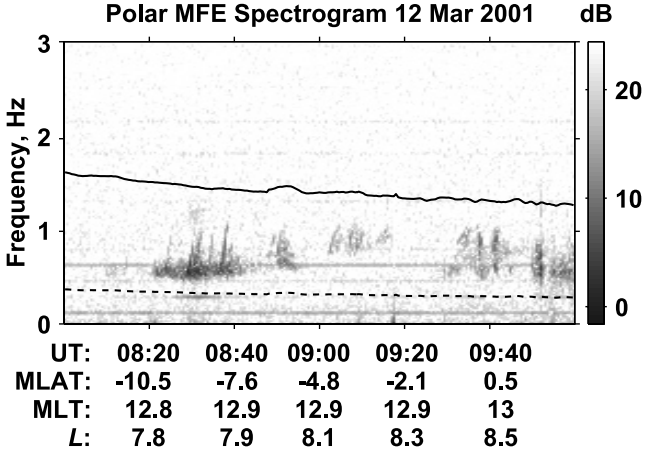

Figure 18. Same as Figure 16 for the segment of the Polar orbit shown in Figure 17.

We also analyzed the solar wind conditions for each of the sixteen detached arc events. There is a preference for the arcs to occur during periods of enhanced dynamic pressure with the average dynamic pressure before and during the arc events about 1.7 times higher than the overall average dynamic pressure for the entire four month study interval. None of the detached arcs were associated with solar wind pressure pulses. There is also a clear trend of southward IMF for up to 8 hours before the detached arc is first observed. This is not surprising given the fact that most of the events occurred during disturbed periods and were associated with plasmaspheric convection plumes. Some arcs appear only after northward turning of the IMF such as was previously described by *Burch et al.* [2002] and *Spasojević et al.* [2004]. This suggests that the equatorward edge of the proton oval may have contributions from ring current-plasmasphere interactions at other times, but the precipitation region does not appear distinct and detached from the main oval unless a northward turning causes the main oval to retreat to higher latitudes. On the other hand, some arc events are still seen in the absence of northward turnings, such that the value of B_z in the hours after the arc is first observed averages to zero in the superposed epoch analysis of all sixteen arc events.

In order to further link the detached proton arcs with wave scattering, we explored Polar MFE observations of EMIC waves during conjunctions with the IMAGE satellite in the March 2001. Two of the previously identified detached arc events occurred during conjunction intervals and MFE observed strong ion cyclotron waves at about the same radial distance as the mapped precipitation region but at an earlier magnetic local time. For the rest of the month, there were no other periods of strong wave activity as Polar crossed the equatorial plane during conjunctions with IMAGE. Also, no other detached arcs were observed in the absence of waves.

9. CONCLUSIONS

It has long been recognized that energetic protons could be precipitated from the ring current as a result of wave-particle interactions occurring within the duskside plasmasphere. Imaging of the proton aurora and plasmasphere has allowed

us to extend previous observational work by exploring this process from a global perspective. We find that arcs of precipitating protons which occur in the afternoon local time sector equatorward of and detached from the main proton auroral oval during geomagnetic disturbances are consistently associated with sunward extending regions of cold plasma or plasmaspheric plumes. We continue to explore the occurrence of electromagnetic ion cyclotron waves in association with the precipitating protons by means of *in situ* observations presented here as well as the ground based measurements reported by *Immel et al.* [this volume]. Finally, the afternoon subauroral proton arcs provide an excellent basis for comparison with predicted proton precipitation patterns from wave scattering included in the increasingly sophisticated global ring current models.

Acknowledgments. We are grateful to Kyoto World Data Center for providing the geomagnetic indices, the ACE MAG and SWEPAM instrument teams, the ACE Science Center, the CDAWeb, and R. Lepping and K. Oglivie at NASA for providing the solar wind data. The work at Los Alamos was conducted under the auspices of the U.S. Department of Energy. The work at UCLA was supported by NASA contract NAG 5-3171. The work at Univ. of Arizona was supported by a subcontract from Southwest Research Institutte, under NASA contract NAS5-96020.

REFERENCES

Anderson B. J., R. E. Erlandson, and L. J. Zanetti (1992), A statistical study of Pc 1-2 magnetic pulsations in the equatorial magnetosphere. 1. Equatorial occurrence distributions., *J. Geophys. Res., 97*(A3), 3075–3088.

Bame, S. J., et al. (1993), Magnetospheric plasma analyzer for spacecraft with constrained resources, *Rev. Sci. Instrum., 64* 1026–1033.

Burch, J. L. (2000), IMAGE mission overview, *Space Sci. Rev., 91*, 1–14.

Burch, J. L., D. G. Mitchell, B. R. Sandel, P. C. Brandt, and M. Wuest (2001), Global dynamics of the plasmasphere and ring current during magnetic storms, *Geophys. Res. Lett., 28*(6), 1159–1162.

Burch, J. L., et al. (2002), Interplanetary magnetic field control of afternoon- sector detached proton auroral arcs, *J. Geophys. Res., 107*(A9), 1251, doi:10.1029/2001JA007554.

Carpenter D. L. (1970), Whistler evidence of the dynamic behaviour of the duskside bulge in the plasmasphere. *J. Geophys. Res., 75*(19), 3837–3847.

Carpenter D. L., B. L. Giles, C. R. Chappell, P. M. E. Decreau, R. R. Anderson, A. M. Persoon, A. J. Smith, Y. Corcuff, and P. Canu (1993), Plasmasphere dynamics in the duskside bulge region: a new look at an old topic, *J. Geophys. Res., 98*(A11), 19243–19271.

Chappell, C. R. (1974), Detached plasma regions in the magnetosphere. *J. Geophys. Res., 79*(13), 1861–1870.

Chen A. J., and R. A. Wolf (192), Effects on the plasmasphere of a time-varying convection electric field. *Planet. Space Sci., 20*(4), 483–509.

Cornwall, J. M., F. V. Coroniti, and R. M. Thorne (1970), Turbulent loss of ring current protons, *J. Geophys. Res., 75*(25), 4699–4709.

Erlandson, R. E., and A. J. Ukhorskiy (2001), Observations of electromagnetic ion cyclotron waves during geomagnetic storms: Wave occurrence and pitch angle scattering, *J. Geophys. Res., 106*(A3), 3883–3896.

Frank, L. A. (1971), Relationship of the plasma sheet, ring current, trapping boundary, and plasmapause near the magnetic equator and local midnight, *J. Geophys. Res., 76*(10), 2265–2275.

Fraser B. J., H. J. Singer, W. J. Hughes, J. R. Wygant, R. R. Anderson, and Y. D. Hu (1996), CRRES Poynting vector observations of electromagnetic ion cyclotron waves near the plasmapause. *J. Geophys. Res., 101*(A7), 15331–15344.

Fraser B. J., and T. S. Nguyen (2001), Is the plasmapause a preferred source region of electromagnetic ion cyclotron waves in the magnetosphere? *J. Atmos. Sol.-Ter. Phys., 63*(11), 1225–1247.

Fok et al., 2005, this volume.

Gary, S. P., M. F. Thomsen, L. Yin, and D. Winske (1995), Electromagnetic proton cyclotron instability: Interactions with magnetospheric protons, *J. Geophys. Res., 100*(A11), 21961–21972.

Goldstein and Sandel, 2005, this volume.

Goldstein, J., M. Spasojević, P. H. Reiff, B. R. Sandel, W. T. Forrester, D. L. Gallagher, and B. W. Reinisch (2003), Identifying the plasmapause in IMAGE EUV data using IMAGE RPI in situ steep density gradients, *J. Geophys. Res., 108*(A4), 1147, doi:10.1029/2002JA009475.

Goldstein, J., B. R. Sandel, M. F. Thomsen, M. Spasojević, and P. H. Reiff (2004), Simultaneous remote sensing and in situ observations of plasmaspheric drainage plumes, *J. Geophys. Res., 109*, A03202, 10.1029/2003JA010281.

Grebowsky, J. M. (1970), Model study of plasmapause motion, *J. Geophys. Res., 75*(22), 4329–4333.

Hubert, B., J. C. Gérard, S. A. Fuselier, and S. B. Mende (2003), Observation of dayside subauroral proton flashes with the IMAGE-FUV imagers, *Geophys. Res. Lett., 30*(3), 1145, doi:10.1029/2002GL016464.

Immel, T. J., S. B. Mende, H. U. Frey, L. M. Peticolas, C. W. Carlson, J.-C. Gérard, B. Hubert, S. A. Fuselier, and J. L. Burch (2002), Precipitation of auroral protons in detached arc, *Geophys. Res. Lett., 29*(11), 1519, doi:10.1029/2001GL013847.

Immel et al., 2005, this volume.

Jaggi R. K., and R. A. Wolf (1973), Self-consistent calculation of the motion of a sheet of ions in the magnetosphere. *J. Geophys. Res., 78*(16), 2852–2866.

Jordanova, V. K., C. J. Farrugia, R. M. Thorne, G. V. Khazanov, G. D. Reeves, and M. F. Thomsen (2001), Modeling ring current proton precipitation by electromagnetic ion cyclotron waves during the May 14–16, 1997, storm, *J. Geophys. Res., 106*(A1), 7–22.

Kennel, C. F. and H. E. Petschek (1966), Limit on stably trapped particle fluxes, *J. Geophys. Res., 71*(A1), 1–27.

Khazanov, G. V., K. V. Gamayunov, and V. K. Jordanova (2003), Self-consistent model of magnetospheric ring current and electromagnetic ion cyclotron waves: The 2–7 May 1998 storm, *J. Geophys. Res., 108*(A12), 1419, doi:10.1029/2003JA009856.

Kintner, P. M and D. A. Gurnett (1977), Observations of ion cyclotron waves within the plasmasphere by Hawkeye 1. *J. Geophys. Res., 82*(16), 2314–2318.

Korth H., M. F. Thomsen, J. E. Borovsky, D. J. McComas (1999), Plasma sheet access to geosynchronous orbit, *J. Geophys. Res., 104*(A11), 25047–25061.

Kozyra, J. U., T. E. Cravens, A. F. Nagy, E. G. Fontheim, and R. S. B. Ong (1984), Effects of energetic heavy ions on electromagnetic ion cyclotron wave generation in the plasmapause region, *J. Geophys. Res., 89*(A4), 2217–2233.

Kozyra, J. U., V. K. Jordanova, R. B. Horne, and R. M. Thorne (1997), Modeling of the contribution of electromagnetic ion cyclotron (EMIC) waves to stormtime ring current erosion, in: *Magnetic Storms*, *Geophys. Monogr. Ser.,* vol 98, edited by B. T. Tsurutani et al., pp. 187–202, AGU, Washington, D. C.

LaBelle, J., R. A. Treumann, W. Baumjohann, G. Haerendel, N. Sckopke, and H. Luhr (1988), *J. Geophys. Res., 93*(A4), 2573–2590.

Lyons, L.R., Thorne R. M. (1972), Parasitic pitch angle diffusion of radiation belt particles by ion cyclotron waves, *J. Geophys. Res., 77*(28), 5608–5616.

Williams D.J., and L. R. Lyons (1974), The proton ring current and its interaction with the plasmapause: Storm recovery phase, *J. Geophys. Res., 79*(28), 4195–4207.

Mauk, B. H. and R. L. McPherron (1980), An experimental test of the electromagnetic ion cyclotron instability within the Earth's magnetosphere, *Phys. Fluids, 23*(10), 211–227.

Mende, S. B., et al. (2000), Far Ultraviolet Imaging from the IMAGE Spacecraft. 3. Spectral Imaging of Lyman-a and OI 135.6 nm, *Space Sci. Rev., 91*, 287–318.

Moldwin M. B., M. F. Thomsen, S. J. Bame, D. McComas, and G. D. Reeves (1995). The fine-scale structure of the outer plasmasphere. *J. Geophys. Res., 100*(A5), 8021–8029.

Mursula K., K. Prikner, F. Z. Feygin, T. Braysy, J. Kangas, R. Kerttula, P. Pollari, T. Pikkarainen T, and O. A. Pokhotelov (2000), Non-stationary Alfven resonator: new results on Pc 1 pearls and IPDP events. *J. Atmos. Sol.-Ter. Phys., 62*(4), 299–309.

Russell C. T., R. C. Snare, J. D. Means, D. Pierce, D. Dearborn, M. Larson, G. Barr, G. Le (1995), The GGS/POLAR fields investigation, *Space Sci. Rev., 71*(1–4), 563–582.

Sandel, B. R., et al. (2000), The Extreme Ultraviolet Imager investigation for the IMAGE mission, *Space Sci. Rev., 91*, 197–242.

Sandel, B. R., R. A. King, W. T. Forrester, D. L. Gallagher, A. L. Broadfoot, and C. C. Curtis (2001), Initial Results from the IMAGE Extreme Ultraviolet Imager, *Geophys. Res. Lett., 28*(8), 1439–1442.

Spasojević, M., J. Goldstein, D. L. Carpenter, U. S. Inan, B. R. Sandel, M. B. Moldwin, and B. W. Reinisch (2003), Global response of the plasmasphere to a geomagnetic disturbance, *J. Geophys. Res.*, 108(A9), 1340, doi:10.1029/2003JA009987.

Spasojević, M., H. U. Frey, M. F. Thomsen, S. A. Fuselier, S. P. Gary, B. R. Sandel, and U. S. Inan (2004), The link between a detached subauroral proton arc and a plasmaspheric plume, *Geophys. Res. Lett., 31*, L04803, doi:10.1029/2003GL018389.

Taylor, W. W. L., and L. R. Lyons (1976), Simultaneous equatorial observations of 1- to 30-Hz waves and pitch angle distributions of ring current ions. *J. Geophys. Res., 81*(34), 6177–6183.

Thorne, R. M. and R. B. Horne (1992), The contribution of ion-cyclotron waves to electron heating and SAR-arc excitation near the storm-time plasmapause, *Geophys. Res. Lett., 19*(4), 417–420.

Tsyganenko, N. A., and D. P. Stern (1996), Modeling the global magnetic field of the large-scale Birkeland current systems, *J. Geophys. Res., 101*(A12), 27187–271898.

Yahnina, T. A., A. G. Yahnin, J. Kangas, and J. Manninen (2000), Proton precipitation related to Pc1 pulsations, *Geophys. Res. Lett., 27*(21), 3575–3578.

Young, D. T., S. Perraut, A. Roux, C. De Villedary, R. Gendrin, A. Korth, G. Kremser, and D. Jones (1981), Wave-particle interactions near Ω_{He+} observed on GEOS 1 and 2. I. Propagation of ion cyclotron waves in He^+-rich plasma, *J. Geophys. Res., 86*(A8), 6755–6772.

Zhang, Y., L. J. Paxton, T. J. Immel, H. U. Frey, and S. B. Mende (2002), Sudden solar wind dynamic pressure enhancements and dayside detached auroras: IMAGE and DMSP observations, *J. Geophys. Res., 107*, 8001, doi:10.1029/2002JA009355.

M. Spasojević, Packard Bldg Rm 301, Stanford, CA 94305 USA (maria@nova.stanford.edu)

M. F. Thomsen, Los Alamos National Lab, MS D466, Los Alamos, NM 87544, USA

P. J. Chi, IGPP, UCLA, Box 951567, Los Angeles, CA 90095, USA

B. R. Sandel, Lunar and Planetary Lab, University of Arizona, C. P. Sonett Space Sciences Bldg 63, Tucson, AZ 85721, USA